Linearised Dynamic Analysis of Bimodular Beams

Nahidh H. Kurdi
Civil Engineering Department
College of Engineering – Anbar University

Omar A. Saleh
MSc. Civil Engineering Department
College of Engineering – Anbar University

ABSTRACT.

Linearised dynamic analysis of beams subjected to lateral forces and composed of materials which have different moduli in tension and compression is presented. The position of the neutral surface was rendered independent of the spatial and temporal coordinates by introducing a special assumption which reduced the coupled nonlinear problem of the flexure of such a beam into a linear one. The actual position then became a function of section geometry and the two elastic moduli and was determined by the equivalent section method. The elemental dynamic stiffness matrix was derived using the exact displacement shape functions governed by the governing partial differential equation and the structural stiffness matrix was assembled according to the usual assembling methodology of structural analysis. Symbolic and numerical examples were solved to show the applicability and efficacy of the proposed method.

Key words: **dynamic analysis, bimodular material, equivalent section method, dynamic stiffness matrix, linearization, Euler-Bernoulli beam**.

1. INTRODUCTION.

In traditional application of mechanics of materials theories, it is generally assumed that materials have the same elastic properties in tension and compression, but this is only a simplification, and is not a refined model for the actual behaviour of engineering materials. Many studies have indicated that most materials exhibit different tensile and compressive strains given the same stress applied in tension and compression. Many engineering materials such as concrete, reinforced concrete, metals, graphite, plastics and cord-rubber display such bimodular behaviour [1].

Of a special status for this matter are the composite materials, which are receiving increasing attention in structural applications because of important weight savings. The weight savings emerge as a result of the combination of a light, weak, and flexible matrix material with a very strong and stiff reinforcing material in the form of fibres or granules. One of the important characteristics of composite materials is that they often exhibit different moduli or stiffnesses under tensile loading than those under compressive loading. Thus, large errors may arise if the same modulus assumption is still used. Therefore, it has become a new research trend for many researchers to study the behaviour of structures made of those materials in different contexts.

The first scholar who described the behaviour of members made of those bimodulus, or bimodular materials was Timoshenko [2], but this problem was generally forgotten or ignored up to the beginnings of 1980's of the twentieth century when the revival of interest came from many researchers. Yao and Ye [1] reported that the first scholar who founded an elastic theory of bimodular materials was Ambartsumyan, a Russian scholar. Another researcher, Medri [3], an American scholar, presented a model for the mechanical characterization of isotropic materials with different behaviour in tension and compression. Bert and Tran [4] developed a transfer-matrix method, based on Timoshenko's beam theory for a bimodular beam and applied the method to transient response problems. Reddy [5] presented a finite element method for the transient analysis of bimodular, fibre-reinforced, rectangular plates made of

aramid-rubber and polyester-rubber materials. Rebello et al. [6] studied the vibration of a thick sandwich beam constructed of bimodular material with rectangular cross section and presented both analytical and experimental investigations. Benveniste [7] presented a constitutive theory for transversely isotropic bimodular materials in the framework of large deformations then derived the special case of infinitesimal strains which he used to solve some wave propagation problems. Chen and Juang [8] investigated the dynamic stability of bimodular thick circular and annular plates subjected to a combination of a pure dynamic bending and a uniform dynamic extensional stress in the plane of the plate. Chen *et al.* [9] investigated the dynamic stability of a bimodular beam subjected to a periodic load using the finite element method. Iwase and Hirashima [10] presented an analytical treatment of the dynamic behaviour of beams made of bimodular materials under moving load and determined the natural frequencies and mode shapes of those beams using the transfer matrix method. The same authors, Iwase and Hirashima [11] treated the problem of bending of beams by applying Levinson's beam theory, which include shear deformation and warping of the cross section, to bending analysis of thick rectangular beams made of bimodular materials. Yao and Ye [12] presented an analytical solution for the static bending stresses in a bimodular beam subjected to lateral loading. Another paper of the same authors [13] also contained an analytical solution for bending-compression of a column subjected to combined loading using a flowing coordinate system. Baykara *et al.* [14] presented an analytical solution for the large horizontal and vertical deflections at the free end of a cantilever beam made of a bimodular material under an end moment. Yao and Ye [1] introduced different tension and compression moduli into the analysis of statically indeterminate structures and presented a semi-analytical method for the analysis of these structures. Yao and Wang [15] found analytical solutions for bending-compression and bending-tension members with different moduli under complex stress and subjected to combined loadings. Another paper for Yang and Wang [16] presented an approach to solve dynamic bimodular problems. They used a smoothing technique to avoid the constitutive discontinuity which results from considering the stress-strain curve of bimodular materials as a straight line with a slope discontinuity at the origin. Chen-Zhong [17] presented an analytical solution for the deflection of a geocell with different tension and compression moduli and analyzed the factors affecting the solution of geocell's deflection. Khan *et al.* [18] investigated the effect of bimodularity on free vibration of all edges simply supported, two-layered, cross-ply thick plates using Bert's constitutive material model.

The analysis of structures made of bimodular materials is inherently nonlinear and the exact solutions may not be accessible, especially in dynamic analysis. Therefore, in this study, the linearised dynamic analysis of the flexure of bimodular beams is presented. The procedure proposed in this paper is easy to follow, and practical. To fully delineate this procedure, the dynamic stiffness matrix of a bimodular beam is derived and both symbolic and numerical examples are solved to show the applicability and efficacy of the proposed method.

2. GOVERNING EQUATION OF MOTION.

The governing partial differential equation of transverse vibration of a one-dimensional beam of uniform flexural stiffness, *EI*, under the Euler-Bernoulli kinematical assumptions is

$$EI\frac{\partial^4 u(x,t)}{\partial x^4}+m\frac{\partial^2 u(x,t)}{\partial t^2}=q(x,t) \tag{1}$$

where *EI* is the uniform flexural stiffness, $u(x,t)$ is the transverse displacement of a point on the neutral axis of the beam. The position of this point along the axis is fixed by the spatial coordinate, x. The transverse displacement in a vibration problem is, as evident from the

notation, a function of both position and time. The parameter, m, is commonly said to be the mass per unit length of the beam, but should, more precisely, be called the linear mass density of the beam. The right hand side is the time-varying load.

Variation in section dimensions of the beam, along its axis, introduces only spatial dependence of the product EI whether the problem at hand is a static problem or a dynamic one such as the free or forced transverse vibrations of a beam. Thus for those problems, the governing equation remains a linear partial differential equation, albeit a variable coefficients one. This amounts to the modification of equation (1) to take the form [19]

$$\frac{\partial^4}{\partial x^4}(EI(x)u(x,t)) + m\frac{\partial^2 u(x,t)}{\partial t^2} = q(x,t) \tag{2}$$

Another, rarely-met in practice, situation calls for the modification of equation (2) above to take spatial variation of the linear mass density into consideration. Equation (2), would then take the form

$$\frac{\partial^4}{\partial x^4}(EI(x)u(x,t)) + m(x)\frac{\partial^2 u(x,t)}{\partial t^2} = q(x,t) \tag{3}$$

For the present problem, however, the position of the neutral surface depends on the external force distribution which is in turn made up of the externally applied time-varying loads and the inertia force. The inertia forces are acceleration dependent. Thus the expression of EI becomes dependent on $\partial^2 u/\partial t^2$ such that the governing equation becomes of the form

$$\frac{\partial^4}{\partial x^4}(EI(x,\frac{\partial^2 u}{\partial t^2})u(x,t)) + m(x)\frac{\partial^2 u(x,t)}{\partial t^2} = q(x,t) \tag{4}$$

Equation (4) above has the appearance of a nonlinear partial differential equation but it is, in fact, a nonlinear partial integro-differential equation (Kurdi and Saleh, unpublished work). In this general form, equation (4) is, in all probability, not amenable to solution by separation of variables or other methods of linear analysis, nor yielding for solution in closed form by any other method known to the authors. In order to form a picture for the effect of bimodularity on the dynamic response of beams, linerisation of the governing equation (4) seems a feasible first approach. The linearisation of equation (4) above is presented below. The expression $EI(x,\partial^2 u/\partial t^2)$ is to be replaced by an approximate substitute by the method of equivalent sections so as to replace the nonlinear equation (4) by a linear approximate one. This linearisation will automatically restore the original character of the governing equation, *i.e.* being a partial differential equation, not an integrao-differential one.

In order to substantiate this linearisation, the general expression of EI may be replaced by the corresponding expression of the particular case of pure bending which turned out to be independent of the spatial and temporal coordinates [20, 13].

To complete the linearised analysis, the neutral surface position for pure bending loading case is first derived using the equivalent section method.

Referring to **Fig.(1)**, any section of a beam subject to a pure bending loading condition would be under the action of uniform moment, M. The section height and width are denoted by h and b, respectively. The tensile region height which is the distance down (or up) to the extreme fibre from the neutral surface is h_1, while the compressive region height is h_2. The tensile modulus is denoted by E^t while the compressive modulus is denoted by E^c. Again, tensile and compressive areas are referred to as A^t and A^c, respectively.

The strategy is to convert the compressive area into an equivalent tensile one in the sense of changing the geometry and adopting the tensile modulus, E^t, as the unique modulus of the equivalent section. b_{eq}

The compressive stresses acting on the original and equivalent sections are, respectively

$$\sigma^c = E^c \varepsilon \quad \text{and} \quad \sigma^c_{eq} = E^t \varepsilon_{eq} \tag{5}$$

The pivotal point in what follows is to keep the original and the equivalent section strains the same in order to preserve compatibility. Another (force) condition is to set $N=N_{eq}$, the original and the equivalent compressive force resultants.

These compressive forces, for any stress distribution, is

$$\left.\begin{aligned} N &= \int_{A^c} \sigma^c dA = \int_{A^c} E^c \varepsilon \, dA \\ N_{eq} &= \int_{A^c} \sigma^c_{eq} dA_{eq} = \int_{A^c} E^t \varepsilon_{eq} b_{eq} \, dy \end{aligned}\right\} \tag{6}$$

where b_{eq} , is the equivalent width of the converted section.

Now applying the condition $N=N_{eq}$ and $\varepsilon=\varepsilon_{eq}$ gives

$$b_{eq} = \frac{E^c}{E^t} b \tag{7}$$

First moment around the neutral axis should remain zero.

Thus, $bh_1(h_1/2) = b_{eq}h_2(h_2/2) = (E^c/E^t)bh_2(h_2/2)$, which gives

$$E^c h_2^2 = E^t h_1^2 \tag{8}$$

Equation (8) above together with $h=h_1+h_2$ gives

$$h_1 = \frac{\sqrt{E^c}}{\sqrt{E^t}+\sqrt{E^c}} h, \text{ and } h_2 = \frac{\sqrt{E^t}}{\sqrt{E^t}+\sqrt{E^c}} h \tag{9}$$

Of course, equations (9) are rigorous only for the pure bending case. However, the main assumption of the present work is that they could be used as a first order approximation for the transverse loading case, as was detailed before. By virtue of being independent of the external moment distribution, equations (9) above could be used to linearise the hitherto nonlinear problem.

To do so, a new but, also uniform, equivalent flexural stiffness is calculated as follows: $(EI)_{eq}=E_{eq}I_{eq}$, or $(EI)_{eq} = E^t I_{eq} = E^t[\frac{b}{3}h_1^3 + \frac{b_{eq}}{3}h_2^3]$. Now, equation (7) is invoked to write $(EI)_{eq} = E^t[\frac{b}{3}h_1^3 + \frac{E^c}{3E^t}bh_2^3]$.

Then,

$$(EI)_{eq} = \frac{b}{3}[E^t h_1^3 + E^c h_2^3] \tag{10}$$

Therefore, instead of solving equation (4) in its full nonlinearity, the remaining of this paper will be concerned with solving the following linearised form

$$\frac{b}{3}[E^t h_1^3 + E^c h_2^3]\frac{\partial^4 u(x,t)}{\partial x^4} + m\frac{\partial^2 u(x,t)}{\partial t^2} = q(x,t) \tag{11}$$

where h_1 and h_2 are given by equation (9). In particular, for the free vibration case, equation (11) takes the following form

$$\frac{b}{3}[E^t h_1^3 + E^c h_2^3]\frac{\partial^4 u(x,t)}{\partial x^4} + m\frac{\partial^2 u(x,t)}{\partial t^2} = 0 \tag{12}$$

For brevity, the expression $\frac{b}{3}[E^t h_1^3 + E^c h_2^3]$ in equations (11) and (12) above is denoted by $\overline{EI}$; the equivalent flexural stiffness. Thus for free vibration of a bimodular Euler-Bernoulli beam, the linearised governing equation may be written as

$$\overline{EI}\frac{\partial^4 u(x,t)}{\partial x^4} + m\frac{\partial^2 u(x,t)}{\partial t^2} = 0 \tag{13}$$

Using the method of separation of variables, the solution will be of the form

$$u(x,t) = \psi(x)\phi(t) \tag{14}$$

Substituting the above expression in equation (13) and performing separation of variables, the solution will be

$$\psi(x) = A\sin\beta x + B\cos\beta x + C\sinh\beta x + D\cosh\beta x \tag{15a}$$

$$\phi(t) = Y\sin\kappa t + Z\cos\kappa t \tag{15b}$$

in which

$$\beta^4 = \frac{m\kappa^2}{\overline{EI}} \tag{15c}$$

The general solution is

$$u(x,t) = (Y\sin\kappa t + Z\cos\kappa t)(A\sin\beta x + B\cos\beta x + C\sinh\beta x + D\cosh\beta x) \tag{16}$$

Then for free vibration of a uniform rectangular beam made of bimodular material, the response is given by

$$u(x,t) = (Y\sin\kappa t + Z\cos\kappa t)\left(A\sin\sqrt[4]{\frac{m\kappa^2}{\overline{EI}}}x + B\cos\sqrt[4]{\frac{m\kappa^2}{\overline{EI}}}x + C\sinh\sqrt[4]{\frac{m\kappa^2}{\overline{EI}}}x + D\cosh\sqrt[4]{\frac{m\kappa^2}{\overline{EI}}}x\right) \tag{17}$$

In order to give an impression of the effect of bimodularity on the dynamic response of structures, a symbolic example is given below. The comparison of the natural frequencies in the unimodular and bimodular cases reveals both the extent of the effect of bimodularity and the efficacy of the proposed linearisation in revealing this effect at relatively low computational and conceptual costs.

Symbolic Example 2.1

It is required to determine natural frequencies and mode shapes for the beam shown in **Fig.(2)** below.

For the given problem, the boundary conditions in terms of the transverse displacement could be written as

$$\begin{aligned} \frac{\partial u(0,t)}{\partial x} &= 0, \qquad \frac{\partial^3 u(0,t)}{\partial x^3} = 0 \\ u(L,t) &= 0, \qquad \frac{\partial u(L,t)}{\partial x} = 0 \end{aligned} \tag{E2.1a}$$

Now recalling equation (15a), the above boundary conditions written in terms of $u(x,t)$ imply another set of boundary conditions written in terms of $\psi(x)$ as follows

$$\begin{aligned} \left.\frac{\partial \psi}{\partial x}\right|_{x=0} &= 0, \qquad \left.\frac{\partial^3 \psi}{\partial x^3}\right|_{x=0} = 0 \\ \psi(L) &= 0, \qquad \left.\frac{\partial \psi}{\partial x}\right|_{x=L} = 0 \end{aligned} \tag{E2.1b}$$

The first row in equations (E2.1b) above implies

$$\begin{aligned} A + C &= 0 \\ -A + C &= 0 \end{aligned} \tag{E2.1c}$$

The second row in equation (E2.1b) above implies

$$\begin{aligned} A \sin \beta L + B \cos \beta L + C \sinh \beta L + D \cosh \beta L &= 0 \\ A\beta \cos \beta L - B\beta \sin \beta L + C\beta \cosh \beta L + D\beta \sinh \beta L &= 0 \end{aligned} \tag{E2.1d}$$

where A, B, C and D are the arbitrary constants appearing in equation (15a).

Equations (E2.1c) gives $A = C = 0$. Substituting this into equation (E2.1d) gives

$$\begin{aligned} B \cos \beta L + D \cosh \beta L &= 0 \\ -B\beta \sin \beta L + D\beta \sinh \beta L &= 0 \end{aligned} \tag{E2.1e}$$

Equations (E2.1e) above could be put in a matrix form as follows

$$\begin{bmatrix} \cos \beta L & \cosh \beta L \\ -\beta \sin \beta L & \beta \sinh \beta L \end{bmatrix} \begin{bmatrix} B \\ D \end{bmatrix} = \begin{bmatrix} 0 \\ 0 \end{bmatrix} \tag{E2.1f}$$

To obtain a non-trivial solution of equation (E2.1f) above, *i.e.* a vibrating beam, the determinant of the coefficients matrix in equation (E2.1f) should be set to zero.

$$\begin{vmatrix} \cos\beta L & \cosh\beta L \\ -\beta\sin\beta L & \beta\sinh\beta L \end{vmatrix} = 0 \qquad \text{(E2.1g)}$$

Equation (E2.1g) is known as the frequency equation. This is equivalent to

$$\beta\cos\beta L\sinh\beta L + \beta\sin\beta L\cosh\beta L = 0$$

or

$$\tan\beta L = -\tanh\beta L \qquad \text{(E2.1h)}$$

Equation (E2.1h) is a transcendental equation whose solution cannot be found exactly. An approximation of this solution could be found by trial and error

$$\beta L \approx \frac{3\pi}{4}, \frac{7\pi}{4}, \frac{11\pi}{4}, \cdots \qquad \text{(E2.1i)}$$

or

$$\beta L \approx \frac{(4n-1)}{4}\pi \quad n = 1, 2, 3, \cdots \qquad \text{(E2.1j)}$$

Equation (E2.1j) above is a solution representing an infinity of natural frequencies corresponding to an infinity of mode shapes. Substituting those values of βL into equation (15c) gives

$$\kappa^2 = \frac{\overline{EI}}{m}\left(\frac{4n-1}{4}\right)^4\left(\frac{\pi}{L}\right)^4 \qquad n = 1, 2, 3, \cdots$$

or

$$\kappa = \left(\frac{4n-1}{4}\right)^2\left(\frac{\pi^2}{L^2}\right)\sqrt{\frac{\overline{EI}}{m}} \qquad n = 1, 2, 3, \cdots$$

Then

$$\omega_n^b = \left(\frac{4n-1}{4}\right)^2\left(\frac{\pi}{L}\right)^2\sqrt{\frac{\overline{EI}}{m}} \qquad n = 1, 2, 3, \cdots \qquad \text{(E2.1k)}$$

is an infinity of natural frequencies corresponding to the free vibration of the beam of this example.

If the beam was a unimodular one, using an exactly parallel analysis, the corresponding set of natural frequencies is found to be [21, 19]

$$\omega_n = \left(\frac{4n-1}{4}\right)^2\left(\frac{\pi}{L}\right)^2\sqrt{\frac{EI}{m}} \qquad n = 1, 2, 3, \cdots \qquad \text{(E2.1}l\text{)}$$

Comparing equation E2.1k and E2.1*l*, the ratio ω_n^b / ω_n is found to be

$$\frac{\omega_n^b}{\omega_n} = \sqrt{\frac{\overline{EI}}{EI}} \qquad \text{(E2.1m)}$$

The superscript *b* in ω_n^b above indicates that the natural frequency was computed assuming bimodularity of the beam material. The ratio expressed in equation (E2.1m) above could be substantially simplified as follows: The convention was to choose $E=E^t$, then

$$\overline{EI} = E^t I_{eq} = EI_{eq} \tag{E2.1n}$$

or

$$\overline{EI} = E^t[\frac{b}{3}h_1^3 + \frac{E^c}{E^t}\frac{b}{3}h_2^3]$$

Then

$$\overline{EI} = E(\frac{b}{3})(h_1^3 + \frac{E^c}{E^t}h_2^3)$$

Now we write $\frac{E^c}{E^t} = m_r$, the modular ratio, and remember that $I = \frac{bh^3}{12}$, then

$$\frac{\overline{EI}}{EI} = \frac{E(b/3)(h_1^3 + m_r h_2^3)}{E(b/12)h^3} = 4\left[(\frac{h_1}{h})^3 + m_r(\frac{h_2}{h})^3\right]$$

Then using equation (9)

$$\frac{\overline{EI}}{EI} = 4\left[(\frac{\sqrt{E^c}}{\sqrt{E^t}+\sqrt{E^c}})^3 + m_r(\frac{\sqrt{E^t}}{\sqrt{E^t}+\sqrt{E^c}})^3\right]$$

$$\frac{\overline{EI}}{EI} = 4\left[(\frac{\sqrt{m_r}\sqrt{E}}{\sqrt{E}\left(\sqrt{m_r}+1\right)})^3 + m_r(\frac{\sqrt{E}}{\sqrt{E}\left(\sqrt{m_r}+1\right)})^3\right]$$

$$= 4\left[\frac{m_r\sqrt{m_r}}{\left(\sqrt{m_r}+1\right)^3} + \frac{m_r}{\left(\sqrt{m_r}+1\right)^3}\right]$$

$$= 4\left[\frac{m_r(\sqrt{m_r}+1)}{\left(\sqrt{m_r}+1\right)^3} = \frac{m_r}{\left(\sqrt{m_r}+1\right)^2}\right]$$

$$\therefore \quad \frac{\overline{EI}}{EI} = \frac{4m_r}{\left(\sqrt{m_r}+1\right)^2} \tag{E2.1o}$$

Taking limits as $m_r \to 1$ gives

$$\left.\frac{\overline{EI}}{EI}\right|_{E^c=E^t} = 1 \tag{E2.1p}$$

Equation (E2.1p) above indicates the exactitude of the present analysis despite adopting the assumption of using equation (9) for the location of the neutral surface depth of any beam-column. This is attributable to the fact that axial forces are absent in the present example leading to an exact linear substitute of the governing equation (4).

Now substituting equation (E2.1*o*) into equation (E2.1m) gives

$$\frac{\omega_n^b}{\omega_n} = \frac{2\sqrt{m_r}}{\sqrt{m_r}+1} \tag{E2.1q}$$

Equation (E2.1q) above is quite significant since writing it the other way around; *i.e.* $\omega_n = [(\sqrt{m_r}+1)/(2\sqrt{m_r})]\omega_n^b$, means that ignoring bimodularity of this beam leads to underestimating each natural frequency by the ratio $(\sqrt{m_r}+1)/(2\sqrt{m_r})$ that is less than 1 for $m_r > 1$.

3. A DYNAMIC STIFFNESS MATRIX FOR THE LINEARISED ANALYSIS OF BIMODULAR BEAMS.

So far, the linear partial differential equations governing forced and free vibration of an Euler-Bernoulli beam were modified to produce linearised partial differential equations that govern forced and free vibration of a bimodular Euler-Bernoulli beam. In particular, the free vibration equation was solved subject to a set of boundary conditions to yield natural frequencies, mode shapes and response histories for a bimodular beam corresponding to the given boundary conditions. The effect of bimodularity was already noticeable despite the linearised character of the analysis.

In this section a modification of the standard Euler-Bernoulli dynamic stiffness matrix is given. The modification extends the applicability of this method to the linearised analysis of bimodular beams. In order to start constructing a dynamic stiffness matrix for a bimodular Euler-Bernoulli member, consideration of a general such member is required. **Figure 3** depicts such a member $r\widetilde{s}$ (*i.e.* a bimodular Euler-Bernoulli beam extending between points *r* and *s* on a bimodular structure).

End moments M_r, M_s, and end shears V_r and V_s along with transverse deflections Y_s , Y_r and end rotations θ_r and θ_s are shown in their positive sense in **Fig.(3)**, above.

This is a typical start for constructing a member stiffness matrix by adopting exact shape functions derived from the governing differential equation.

The first three spatial derivatives of the function ψ in (15a) equation are

$$\begin{aligned}
\frac{d\psi(x)}{dx} &= \beta A\cos\beta x - \beta B\sin\beta x + \beta C\cosh\beta x + \beta D\sinh\beta x \\
\frac{d^2\psi(x)}{dx^2} &= -\beta^2 A\sin\beta x - \beta^2 B\cos\beta x + \beta^2 C\sinh\beta x + \beta^2 D\cosh\beta x \\
\frac{d^3\psi(x)}{dx^3} &= -\beta^3 A\cos\beta x + \beta^3 B\sin\beta x + \beta^3 C\cosh\beta x + \beta^3 D\sinh\beta x
\end{aligned} \tag{18}$$

Referring to **Fig.(3)**, the appropriate boundary conditions to be imposed are; supposing $x\big|_r = 0$, $x\big|_s = 0$

$$\begin{aligned}
\left.\frac{d^2\psi}{dx^2}\right|_{x=0} &= -\frac{M_r}{EI}, \text{ and } \left.\frac{d\psi}{dx}\right|_{x=0} = \theta_r \\
\left.\frac{d^3\psi}{dx^3}\right|_{x=0} &= -\frac{V_r}{EI}, \text{ and } \psi\big|_{x=0} = -Y_r
\end{aligned} \tag{19a}$$

It is interesting to note that the first column in equation (19a) contains only force boundary conditions, while the second contains only displacement boundary conditions.

Similarily, boundary conditions for the other end are

$$\left.\frac{d^2\psi}{dx^2}\right|_{x=L} = \frac{M_r}{EI}, \text{ and } \left.\frac{d\psi}{dx}\right|_{x=L} = \theta_s$$
$$\left.\frac{d^3\psi}{dx^3}\right|_{x=L} = -\frac{V_r}{EI}, \text{ and } \left.\psi\right|_{x=L} = Y_s \tag{19b}$$

To build a stiffness relation (the dynamic stiffness matrix in this case) the end forces, M_r, M_s, V_r, V_s need to be expressed in terms of the end displacements; θ_r, θ_s, Y_r and Y_s respectively. Substituting the appropriate values of x into equations (15a) and (18) and using equations (19a) and (19b), this expression could be obtained.

Using the fourth of equations (19a) gives

$$B + D = Y_r \tag{20a}$$

while using the fourth of equation (19b) gives

$$A\sin\beta L + B\cos\beta L + C\sinh\beta L + D\cosh\beta L = Y_s \tag{20b}$$

Using the second row of equations (19a) gives

$$\beta A + \beta C = \theta_r \tag{20c}$$

while using the second row of equations (19b) gives

$$\beta A\cos\beta L - \beta B\sin\beta L + \beta C\cosh\beta L + \beta D\sinh\beta L = \theta_s \tag{20d}$$

Equations (20a, b, c and d) could be cast in the following matrix form

$$\begin{bmatrix} \beta & 0 & \beta & 0 \\ \beta\cos\beta L & -\beta\sin\beta L & \beta\cosh\beta L & \beta\sinh\beta L \\ 0 & 1 & 0 & 1 \\ \sin\beta L & \cos\beta L & \sinh\beta L & \cosh\beta L \end{bmatrix} \begin{bmatrix} A \\ B \\ C \\ D \end{bmatrix} = \begin{bmatrix} \theta_r \\ \theta_s \\ \psi_r \\ \psi_s \end{bmatrix} \tag{21}$$

or more concisely

$$SR_c = D_c \tag{22}$$

inverting S systematically, we obtain

$$R_c = \mathrm{S}^{-1} D_c \tag{23}$$

Performing the symbolic inversion by hand or by a computer algebra package; like Maple, we find that

$$\begin{bmatrix} A \\ B \\ C \\ D \end{bmatrix} = S^{-1} \begin{bmatrix} \theta_r \\ \theta_s \\ \psi_r \\ \psi_s \end{bmatrix} \tag{24}$$

where

$$S^{-1}(1,1) = \frac{1 - \sinh\beta L \sin\beta L - \cos\beta L \cosh\beta L}{2\beta(1 - \cosh\beta L \cos\beta L)}$$

$$S^{-1}(1,2) = \frac{\cos\beta L - \cosh\beta L}{2\beta(1 - \cosh\beta L \cos\beta L)}$$

$$S^{-1}(1,3) = \frac{\cos\beta L \sinh\beta L + \cosh\beta L \sin\beta L}{2(1 - \cosh\beta L \cos\beta L)}$$

$$S^{-1}(1,4) = \frac{\sin\beta L + \sinh\beta L}{2(1 - \cosh\beta L \cos\beta L)}$$

$$S^{-1}(2,1) = \frac{\cosh\beta L \sin\beta L - \sinh\beta L \cos\beta L}{2\beta(1 - \cosh\beta L \cos\beta L)}$$

$$S^{-1}(2,2) = \frac{\sinh\beta L - \sin\beta L}{2\beta(1 - \cosh\beta L \cos\beta L)}$$

$$S^{-1}(2,3) = \frac{\cosh\beta L \cos\beta L - \sinh\beta L \sin\beta L - 1}{2(1 - \cosh\beta L \cos\beta L)}$$

$$S^{-1}(2,4) = \frac{\cos\beta L - \cosh\beta L}{2(1 - \cosh\beta L \cos\beta L)}$$

$$S^{-1}(3,1) = \frac{1 + \sinh\beta L \sin\beta L - \cos\beta L \cosh\beta L}{2\beta(1 - \cosh\beta L \cos\beta L)}$$

$$S^{-1}(3,2) = \frac{\cosh\beta L - \cos\beta L}{2\beta(1 - \cosh\beta L \cos\beta L)}$$

$$S^{-1}(3,3) = \frac{-\cos\beta L \sinh\beta L - \cosh\beta L \sin\beta L}{2(1 - \cosh\beta L \cos\beta L)}$$

$$S^{-1}(3,4) = \frac{-\sin\beta L - \sinh\beta L}{2(1 - \cosh\beta L \cos\beta L)}$$

$$S^{-1}(4,1) = \frac{\cos\beta L \sinh\beta L - \cosh\beta L \sin\beta L}{2\beta(1 - \cosh\beta L \cos\beta L)}$$

$$S^{-1}(4,2) = \frac{\sin\beta L - \sinh\beta L}{2\beta(1 - \cosh\beta L \cos\beta L)}$$

$$S^{-1}(4,3) = \frac{\sinh\beta L \sin\beta L - \cos\beta L \cosh\beta L - 1}{2(1 - \cosh\beta L \cos\beta L)}$$

$$S^{-1}(4,4) = \frac{\cosh\beta L - \cos\beta L}{2(1 - \cosh\beta L \cos\beta L)}$$

In a similar fashion, one may produce the following force-arbitrary constants relationship

$$\begin{bmatrix} 0 & \beta^2 & 0 & \beta^2 \\ -\beta^2\sin\beta L & -\beta^2\cos\beta L & \beta^2\sinh\beta L & \beta^2\cosh\beta L \\ -\beta^3 & 0 & \beta^3 & 0 \\ -\beta^3\cos\beta L & \beta^3\sin\beta L & \beta^3\cosh\beta L & \beta^3\sinh\beta L \end{bmatrix} \begin{bmatrix} A \\ B \\ C \\ D \end{bmatrix} = \frac{1}{\overline{EI}} \begin{bmatrix} -M_r \\ M_s \\ -V_r \\ -V_s \end{bmatrix} \tag{25}$$

or more concisely

$$(\overline{EI})\bar{S}R_c = F_c \tag{26}$$

Now our original aim was to write the force column, F_c, in terms of the displacement column, D_c. But $F_c = (\overline{EI})\bar{S}R_c$, from equation (26). Substituting for R_c from equation (23) gives

$$F_c = (\overline{EI})\bar{S}S^{-1}D_c \tag{27}$$

Performing the multiplication $(\overline{EI})\bar{S}S^{-1}$ involved in equation (27) above systematically gives a dynamic stiffness matrix for a bimodular Euler-Bernoulli beam.

$$K_e^b = (\overline{EI})\bar{S}S^{-1} \tag{28}$$

The resulting elements of this elemental dynamic stiffness matrix are

$$\begin{aligned}
K_e^b(1,1) &= \frac{\sinh\beta L\cos\beta L - \cosh\beta L\sin\beta L}{\left[(\cosh\beta L\cos\beta L - 1)L\right]/\beta L\,\overline{EI}} \\
K_e^b(1,2) &= \frac{\sin\beta L + \sinh\beta L}{\left[(\cosh\beta L\cos\beta L - 1)L\right]/\beta L\,\overline{EI}} \\
K_e^b(1,3) &= \frac{\beta\sinh\beta L\sin\beta L}{\left[(\cosh\beta L\cos\beta L - 1)L\right]/\beta L\,\overline{EI}} \\
K_e^b(1,4) &= \frac{\beta(\cosh\beta L - \cos\beta L)}{\left[(\cosh\beta L\cos\beta L - 1)L\right]/\beta L\,\overline{EI}} \\
K_e^b(2,2) &= \frac{\sinh\beta L\cos\beta L - \cosh\beta L\sin\beta L}{\left[(\cosh\beta L\cos\beta L - 1)L\right]/\beta L\,\overline{EI}} \\
K_e^b(2,3) &= \frac{\beta(\cosh\beta L - \cos\beta L)}{\left[(\cosh\beta L\cos\beta L - 1)L\right]/\beta L\,\overline{EI}} \\
K_e^b(1,3) &= \frac{\beta\sinh\beta L\sin\beta L}{\left[(\cosh\beta L\cos\beta L - 1)L\right]/\beta L\,\overline{EI}} \\
K_e^b(3,3) &= \frac{\beta^2(-\sinh\beta L\cos\beta L - \cosh\beta L\sin\beta L)}{\left[(\cosh\beta L\cos\beta L - 1)L\right]/\beta L\,\overline{EI}} \\
K_e^b(3,4) &= \frac{\beta^2(-\sinh\beta L - \sin\beta L)}{\left[(\cosh\beta L\cos\beta L - 1)L\right]/\beta L\,\overline{EI}} \\
K_e^b(4,4) &= \frac{\beta^2(-\sinh\beta L\cos\beta L - \cosh\beta L\sin\beta L)}{\left[(\cosh\beta L\cos\beta L - 1)L\right]/\beta L\,\overline{EI}}
\end{aligned} \tag{29}$$

Thus, the element stiffness matrix may be written as

$$\begin{bmatrix} M_r \\ M_s \\ V_r \\ V_s \end{bmatrix} = \begin{bmatrix} K^b_{e\,11} & K^b_{e\,12} & K^b_{e\,13} & K^b_{e\,14} \\ K^b_{e\,21} & K^b_{e\,22} & K^b_{e\,23} & K^b_{e\,24} \\ K^b_{e\,31} & K^b_{e\,32} & K^b_{e\,33} & K^b_{e\,34} \\ K^b_{e\,41} & K^b_{e\,42} & K^b_{e\,43} & K^b_{e\,44} \end{bmatrix} \begin{bmatrix} \theta_r \\ \theta_s \\ Y_r \\ Y_s \end{bmatrix} \tag{30}$$

Numerical Example 3.1

The two-span beam shown in **Fig.(4)** is subjected to the external dynamic loading $q = 25\sin \omega t$ as indicated. We find the internal moments of the beam and the maximum normal stresses at the fixed end for the given forcing frequency =120 *rad*/*sec*. We choose the bimodular ratios E^t/E^c= 2, 3, 4, 5, 6 and E^t/E^c= 1/2, 1/3, 1/4, 1/5, 1/6 and use the same modulus assumption for comparison. Let L_1=L_2=3m, m_1=m_2=0.192 kN.sec^2/m^2, E= 2×10^7 kN/m^2 and cross section dimensions of $0.2m \times 0.4m$.

Referring to the free body diagram shown in **Fig.(4b)**, the structural dynamic stiffness matrix is

$$\begin{bmatrix} M^{ext}_B \\ M^{ext}_C \end{bmatrix} = \begin{bmatrix} KB^2_{11} + KB^2_{22} & KB^2_{12} \\ KB^2_{12} & KB^2_{22} \end{bmatrix} \begin{bmatrix} R^{ext}_B \\ R^{ext}_C \end{bmatrix} \tag{E3.1a}$$

in which the stiffness coefficients are given by equations (29) and the superscripts represent the number of structural member.

Using the harmonic frequency =120 *rad*/*sec* gives the frequency parameter

$$\beta = \sqrt{\frac{m\omega^2}{EI}} = 0.599 \text{ for } E^t = E^c$$

Thus,

$$\beta L = 1.797$$

Therefore, the stiffness matrix will be as follows

$$\begin{bmatrix} M^{ext}_B \\ M^{ext}_C \end{bmatrix} = \begin{bmatrix} 7.797(\frac{EI}{L}) & 2.076(\frac{EI}{L}) \\ 2.076(\frac{EI}{L}) & 3.898(\frac{EI}{L}) \end{bmatrix} \begin{bmatrix} R^{ext}_B \\ R^{ext}_C \end{bmatrix} \tag{E3.1b}$$

But for the analysis, the external loading must be transformed to the equivalent end moments as M^F_B and M^F_C which may be calculated as follows:

According to the governing partial differential equation of motion,

$$EI\frac{\partial^4 u(x,t)}{\partial x^4} + m\frac{\partial^2 u(x,t)}{\partial t^2} = q(x,t)$$

Using the separation of variables and concentrating on the spatial factor of the produced general solution, the following ordinary differential equation is obtained

$$\frac{d^4\psi}{dx^4} - \beta^4\psi = \frac{q(x)}{EI}$$

But, because the applied loading is uniform, this equation becomes

$$\frac{d^4\psi}{dx^4} - \beta^4\psi = \frac{q}{EI} \tag{E3.1c}$$

The solution of equation above consists of the homogeneous solution ψ_h and the particular solution ψ_p. The particular solution ψ_p can be obtained by trying the following polynomial equation

$$\psi_p = C_1x^4 + C_2x^3 + C_3x^2 + C_4x + C_5 \tag{E3.1d}$$

Substituting ψ_p into equation (E3.1c) yields

$$(24 - \beta^4x^4)C_1 - \beta^4(C_2x^3 + C_3x^2 + C_4x + C_5) = \frac{q}{EI}$$

Comparing both sides of the above equation gives

$$C_1 = C_2 = C_3 = C_4 = 0, C_5 = -\frac{q}{\beta^4 EI} \tag{E3.1e}$$

Thus, the complete solution of equation (E3.1c) is

$$\psi = \psi_h + \psi_p = A\sin\ \beta x + B\cos\ \beta x + C\sinh\ \beta x + D\cosh\ \beta x - \frac{q}{\beta^4 EI} \tag{E3.1f}$$

To obtain fixed end moments, the pinned ends at *B* and *C* are set as fixed end supports. Substituting the boundary conditions in the equation (E3.1f) above, the arbitrary constants *A*, *B*, *C* and *D* are found to be

$$\begin{aligned}
A &= \frac{q}{EI\beta^4}\left[\frac{\sin\ \beta L + \sinh\ \beta L - \cos\ \beta L\sinh\ \beta L - \cosh\ \beta L\sin\ \beta L}{2 - 2\cos\ \beta L\cosh\ \beta L}\right] \\
B &= \frac{q}{EI\beta^4}\left[\frac{1 + \cos\ \beta L - \cosh\ \beta L - \cos\ \beta L\cosh\ \beta L + \sin\ \beta L\sinh\ \beta L}{2 - 2\cos\ \beta L\cosh\ \beta L}\right] \\
C &= \frac{q}{EI\beta^4}\left[\frac{\cos\ \beta L\sinh\ \beta L + \sin\ \beta L\cosh\ \beta L - \sin\ \beta L - \sinh\ \beta L}{2 - 2\cos\ \beta L\cosh\ \beta L}\right] \\
D &= \frac{q}{EI\beta^4}\left[\frac{1 - \cos\ \beta L\cosh\ \beta L - \sin\ \beta L\sinh\ \beta L - \cos\ \beta L + \cosh\ \beta L}{2 - 2\cos\ \beta L\cosh\ \beta L}\right]
\end{aligned} \tag{E3.1g}$$

The fixed-end moments can be calculated by applying the following relationships

$$\left.\frac{d^2\psi}{dx^2}\right|_{x=0} = -\frac{M_B^F}{EI} \quad \text{and} \quad \left.\frac{d^2\psi}{dx^2}\right|_{x=L} = \frac{M_C^F}{EI}$$

Using equation (E3.1f) along with the above equations gives M_B^F and M_C^F expressed in terms of *A*, *B*, *C* and *D* as given by equation (E3.1g). Consequently, the fixed-end moments are

$$M_B^F = \frac{qL^2}{(\beta L)^2}\left[\frac{\cosh\beta L - \cos\beta L - \sin\beta L\sinh\beta L}{\cos\beta L\cosh\beta L - 1}\right] \tag{E3.1h}$$

$$M_B^F = -M_C^F$$

Accordingly,

$$\begin{bmatrix} M_B^F \\ M_C^F \end{bmatrix} = \begin{bmatrix} -19.106 \\ 19.106 \end{bmatrix}$$

Substituting into equation (E3.1b) and taking the inverse of the stiffness matrix and multiplying by the fixed-end moments gives the rotational displacements at joint *B* and *C*, as follows

$$\begin{bmatrix} R_B^{ext} \\ R_C^{ext} \end{bmatrix} = \begin{bmatrix} 0.298931 & -0.07959 \\ -0.07959 & 0.149446 \end{bmatrix} \frac{L}{EI} \begin{bmatrix} -19.106 \\ +19.106 \end{bmatrix} = \begin{bmatrix} 7.232069 \\ -4.37601 \end{bmatrix} \frac{L}{EI} \tag{E3.1i}$$

The internal moments can be evaluated as follows

$$\begin{bmatrix} M_1 \\ M_2 \\ M_3 \\ M_4 \end{bmatrix} = \begin{bmatrix} KB_{12}(R_B) \\ KB_{22}(R_B) \\ KB_{11}(R_B) + KB_{12}(R_C) + M_B^F \\ KB_{21}(R_B) + KB_{22}(R_C) + M_C^F \end{bmatrix} \begin{bmatrix} 15.013 \\ 28.197 \\ -28.197 \\ 0 \end{bmatrix} \tag{E3.1j}$$

and the normal stresses at the fixed end can be calculated as follows

$$\begin{aligned} \sigma^t &= \frac{My}{I} = \frac{3My}{b\left(h_1^3 + \frac{E^c}{E^t} h_2^3\right)} \\ &= \frac{3E^t My}{b\left(E^t h_1^3 + E^c h_2^3\right)} = \frac{E^t}{EI} My \end{aligned} \tag{E3.1k}$$

Similarly

$$\sigma^c = \frac{E^c}{EI} My$$

Thus, for $E^t = E^c$

$$\sigma^t = 2.814 Mpa$$

and

$$\sigma^c = 2.814 Mpa$$

Taking other bimodular ratios and following the same procedure presented above, results of the analysis when the bimodular ratio varies as E^t/E^c=1,2, ..., 6 and E^t/E^c=1, 1/2, ..., 1/6 are obtained. The results are listed in **Table(1)**. Results for rotational displacements, internal moments and extreme fibre stresses are maxima of the spatial factors in the complete solution. The complete solution is obtained by multiplying those values by the harmonic temporal factor $Y\sin\kappa t + Z\cos\kappa t$ the arbitrary constants of which are fixed by initial conditions.

Figs.(5-19) give pictorial representation for the results in the **Table(1)** below. Time histories, in particular, show the effect of bimodularity on the different responses. It is obvious from these figures that changing the bimodular ratio changes the magnitude of the response in a pointwise fashion, but the character of the response remain the same. All the responses reflect the linearised character of the analysis. In particular, it is easily seen that a harmonic forcing produced only harmonic responses for all bimodular ratios. No subharmonic or superharmonic responses are seen, which is a peculiarity of linear analysis.

4. CONCLUSION.

The originally nonlinear equation, governing the vibrations of bimodular beams was linearised by adopting the equations giving the neutral surface position of a beam under pure

bending for the general transverse loading case. A symbolic example was solved in which a formula for the ratio between successive natural frequencies in the bimodular and the unimodular cases was derived. The formula gave the magnitude of error expected in estimating natural frequencies if bimodularity was ignored. The elemental dynamic stiffness matrix corresponding to the given linearised governing equation was derived. This matrix was used to assemble a structural dynamic stiffness matrix for an example continuous beam the dynamic responses of which under harmonic load were shown to be significantly affected by the modular ratio. The responses remained, however, linear in character as was shown by the absence of superharmonic or subharmonic responses for harmonic input.

5. REFERENCES

[1] Yao, W. J., and Ye, Z. M., "Internal forces for statically indeterminate structures having different moduli in tension and compression," Journal of Engineering Mechanics, **132**(7), 739-746, 2006.

[2] Timoshenko, S., Strength of Materials, Part II, Advanced Theory and Problems, Van Nostrand Company, Princeton, 1941.

[3] Medri, G., "A nonlinear elastic model for isotropic materials with different behaviour in tension and compression," Journal of Engineering Materials and Technology, **104**(January), 26-28, 1982.

[4] Bert, C. W. and Tran, A. D., "Transient response of a thick beam of bimodular materials," Earthquake Engineering and Structural Dynamics, **10**(3), 551-560, 1982.

[5] Reddy, J. N., "Transient response of laminated-material, composite rectangular plates," Journal of Composite Materials, **16**(139), 139-152, 1982.

[6] Rebello, C. A., Bert, C. W., and Gordaninejad, F., "Vibrations of bimodular sandwich beams with thick facings: A new theory and experimental results," Journal of Sound and Vibration, **90**(3), 381-397, 1983.

[7] Benveniste, Y., "A Constitutive Theory for Transversely Isotropic Bimodulus Materials with a Class of Steady Wave Solutions," Acta Mechanica, **46**(1-4), 137-153, 1983.

[8] Chen, L. W., and Juang, D. P., "Axisymmetric dynamic stability of a bimodulus thick circular plate," Computers and Structures, **41**(2), 257-263, 1987.

[9] Chen, L. Y., Lin, P. D., and Chen, L. W., "Dynamic stability of thick bimodulus beams," Computers and Structures, **26**(6), 933-939, 1991.

[10] Iwase, T., and Hirashima, K. I., "Dynamic response analysis of thick rectangular beam made of bimodulus materials," The Japan Society of Mechanical Engineers, **63**(96), 109-117, 1997.

[11] Iwase, T., and Hirashima, K. I., "High-accuracy analysis of beams of bimodulus materials," Journal of Engineering Mechanics, **126**(2), 149-156, 2000.

[12] Yao, W. J., and Ye, Z. M., "Analytical solution for bending beam subject to lateral force with different modulus," Applied Mathematics and Mechanics, **25**(10), 1107-1117, 2004a.

[13] Yao, W. J., and Ye, Z. M., "Analytical solution of bending-compression column using different tension-compression modulus," Applied Mathematics and Mechanics, **25**(9), 983-993, 2004b.

[14] Baykara, C., Guven, U., and Bayer, I., "Large deflections of a cantilever beam of nonlinear bimodulus material subjected to an end moment," *Journal of Reinforced Plastics and Composites*, **24**(12), 1321-1326, 2005.

[15] Yao, W. J., and Wang, X., "Analytic solution for bending-compression/tension members with different moduli," *Journal of Physics: Conference Series* 96, 012025, 2008.

[16] Yang, H., and Wang, B., "An analysis of longitudinal vibration of bimodular rod via

smoothing function approach," Journal of Sound and Vibration, **317**(3-5), 419-431, 2008.
[17] Chen-zhong, Q., "Deformation of geocell with different tensile and compressive modulus," *EJGE*, 14(6), 1-14, 2009.
[18] Khan, K., Patel, B. P., and Nath, Y., "Free vibration analysis of bimodular material laminated thick plates using an efficient individual layer theory," 14th national conference on machines and mechanisms (NaCoMM09), NIT, Durgapur, India, December 17-18, 353-359, 2009.
[19] Clough, R. W., and Penzien, J., Dynamics of Structures, Computers & Structures, Inc., New York, 2003.
[20] He, X. T., Chen, S. L., and Sun, J. Y., "Applying the equivalent section method to solve beam subjected to lateral force and bending-compression column with different moduli," International Journal of Mechanical Sciences, 49(7), 919-924, 2007.
[21] Cheng, F. Y., Matrix Analysis of Structural Dynamics: Applications and Earthquake Engineering, Marcel Dekker, Inc., New York, 2001.

Table(1): Results of analysing the continuous beam of Example 3.1 for different modular ratios.

E^c/E^t	h_1(m)	h_2(m)	Flexural Stiffness (kN.m^2)	Rotational Displacements (rad)		Internal Moments (kN.m)				σ^t (MPa)	σ^c (MPa)
				$R_c^{ext}\times10^{-3}$	$R_c^{ext}\times10^{-3}$	M_1	M_2	M_3	M_4		
6	0.115	0.285	7120.6	3.6420	-2.2460	19.38	32.60	-32.60	0	6.259	2.559
5	0.123	0.277	8148.8	3.0666	-1.8830	18.40	31.64	-31.64	0	5.554	2.501
4	0.133	0.267	9481.5	2.5428	-1. 5562	17.48	30.74	-30.74	0	4.903	2.461
3	0.146	0.253	11643.21	2.0023	-1.2212	16.67	29.91	-29.91	0	4.180	2.426
2	0.165	0.234	14641.41	1.5391	-0.9352	15.87	29.09	-29.09	0	3.576	2.536
1	0.2	0.2	21333.34	1.0170	-0.6153	15.01	28.19	-28.19	0	2.814	2.814
1/2	0.234	0.165	29281.03	0.7248	-0.4375	14.53	27.67	-27.67	0	2.322	3.275
1/3	0.253	0.146	34298.40	0.6135	-0.3696	14.30	27.46	-27.46	0	2.109	3.652
1/4	0.267	0.133	37927.31	0.5520	-0.3327	14.23	27.36	-27.36	0	1.996	3.992
1/5	0.277	0.123	40743.6	0.5129	-0.3090	14.20	27.32	-27.32	0	1.930	4.286
1/6	0.285	0.115	43028.9	0.4836	-0.2912	14.082	27.21	-27.21	0	1.858	4.515

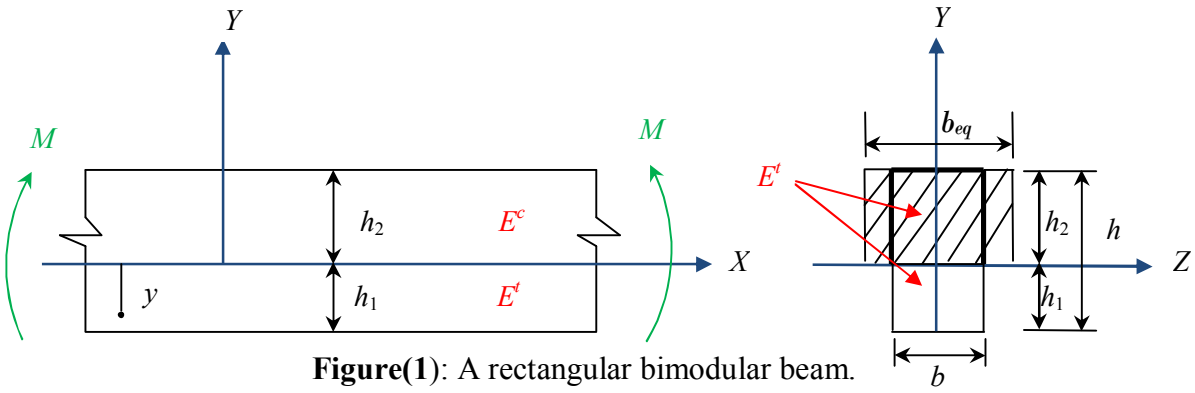

Figure(1): A rectangular bimodular beam.

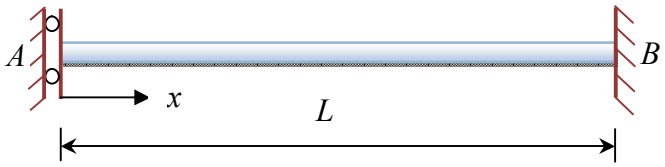

Figure (2): The beam of symbolic example 2.1.

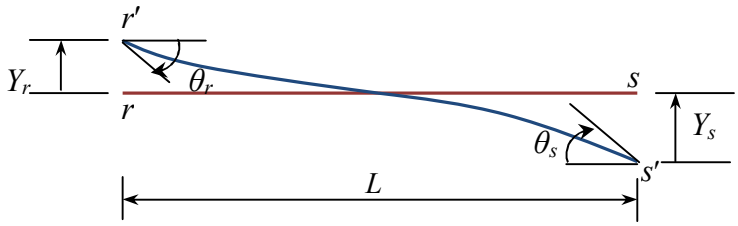

(a): Deformed configuration.

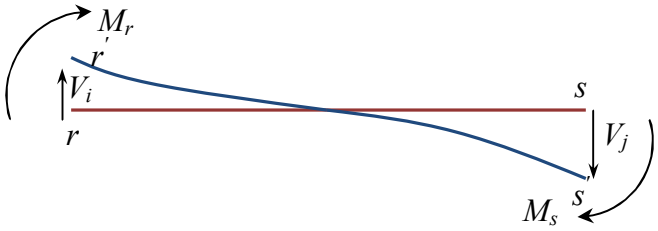

(b): End forces.

Figure (3): Typical deformed beam.

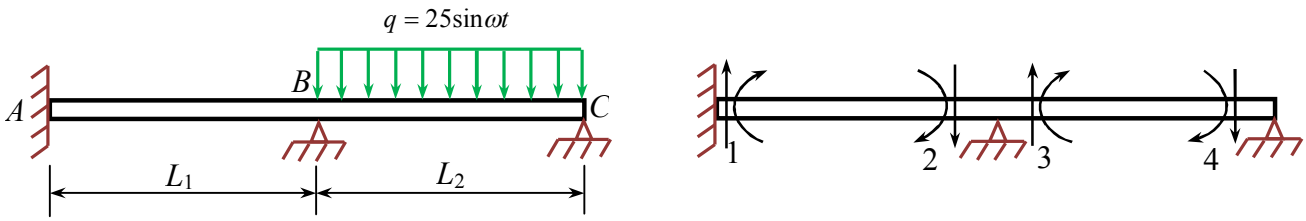

(a). The given beam

(b). Internal actions

Figure (4): A continuous two span beam under dynamic loading.

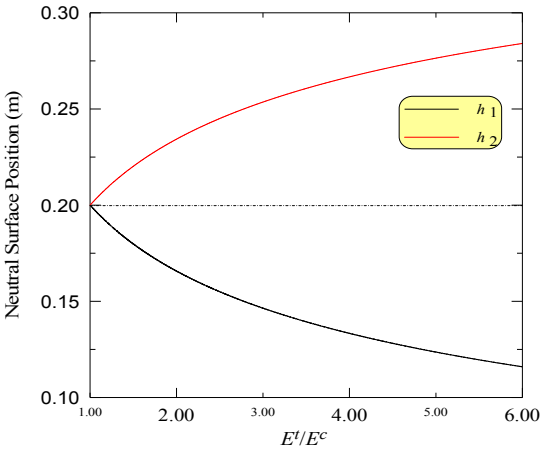

Figure (5): Variation of tension and compression region heights with E^t/E^c.

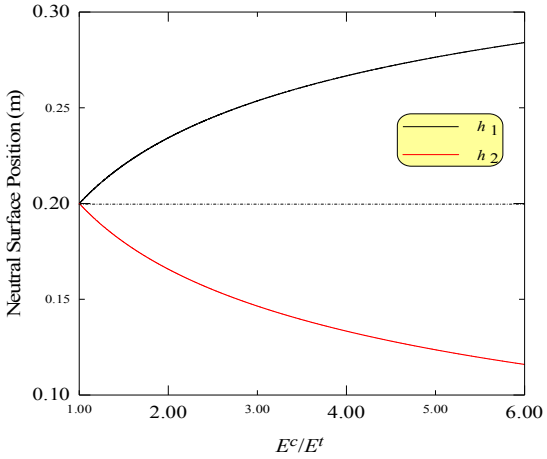

Figure (6): Variation of tension and compression regions height with E^c/E^t.

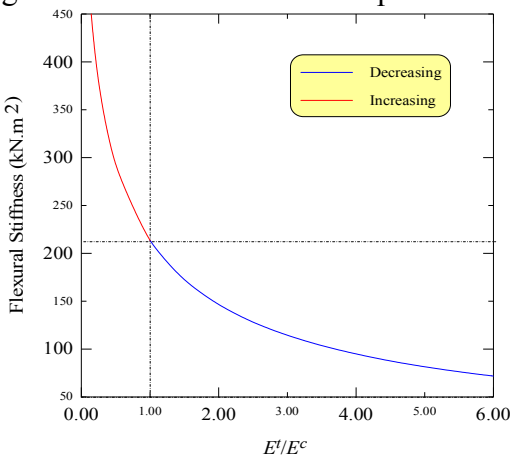

Figure (7): Variation of flexural stiffness with different bimodular ratios.

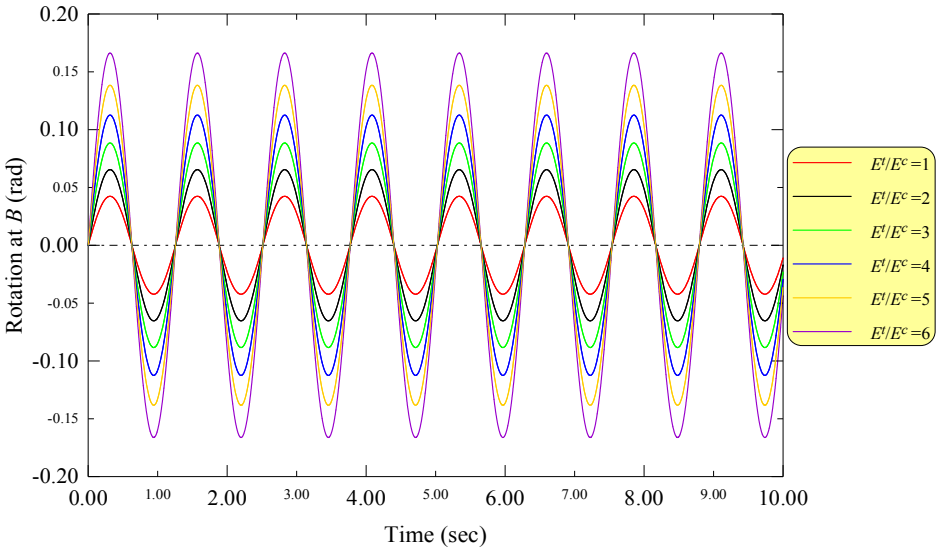

Figure (8): Time histories of rotational displacement at point B for different E^t/E^c ratios..

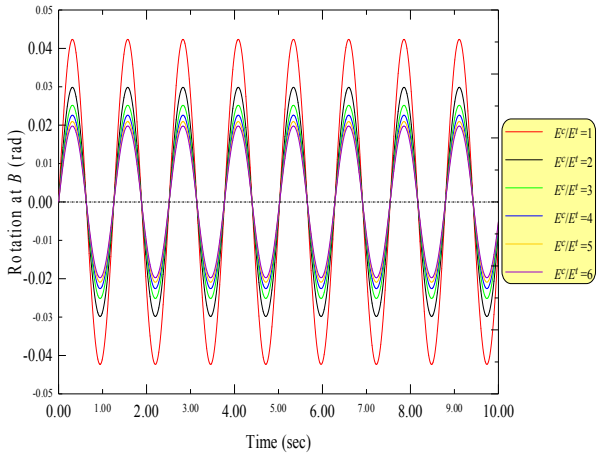

Figure (9): Time histories of rotational displacement at point B for different E^c/E^t ratios.

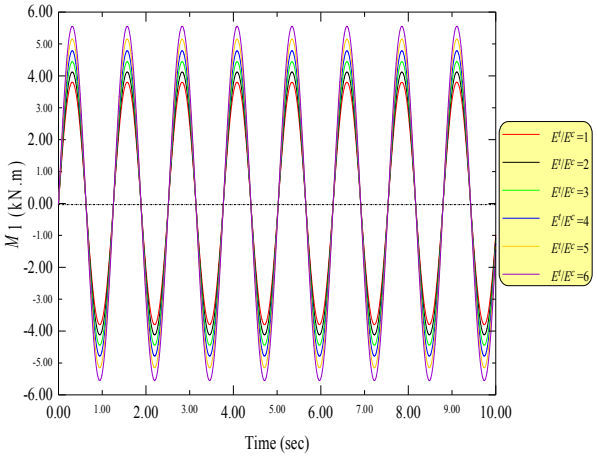

Figure (10): Time histories of internal moment M_1 for different E^t/E^c ratios.

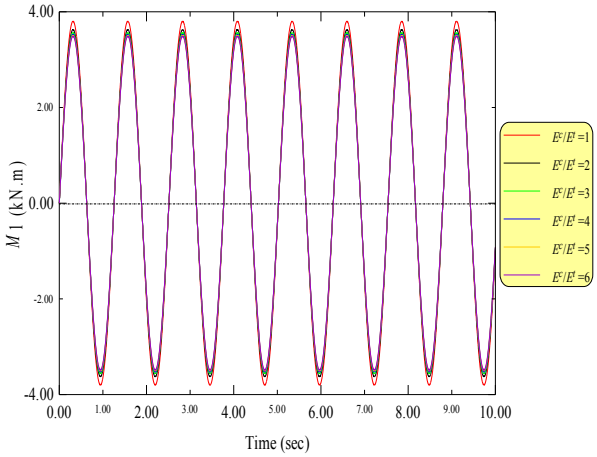

Figure (11): Time histories of internal moment M_1 for different E^c/E^t ratios.

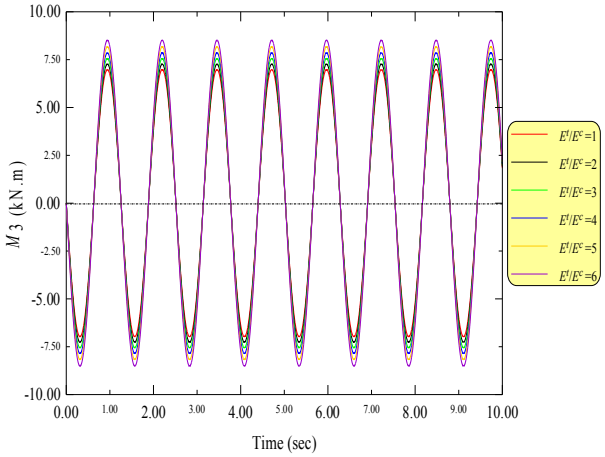

Figure (12): Time histories of internal moment M_3 for different E^t/E^c ratios.

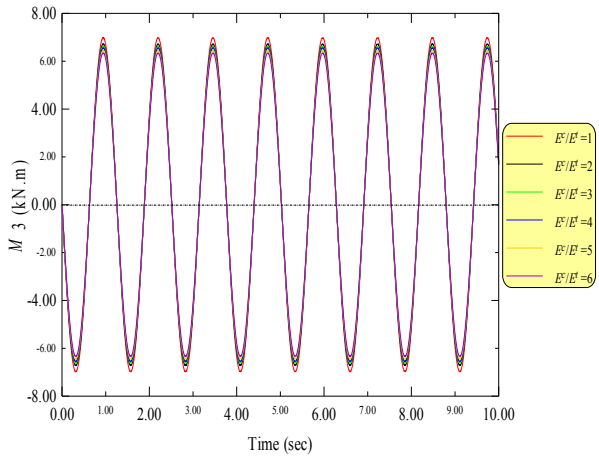

Figure (13): Time histories of internal moment M_3 for different E^c/E^t ratios.

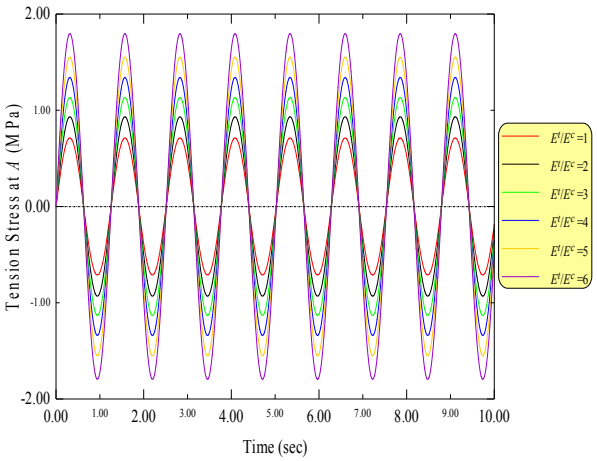

Figure (14): Time histories of the extreme-fibre tension stress for different E^t/E^c ratios.

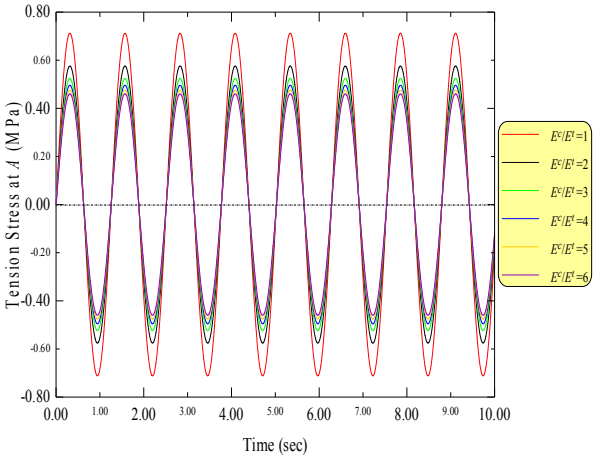

Figure (15): Time histories of the extreme-fibre tension stress for different E^c/E^t ratios.

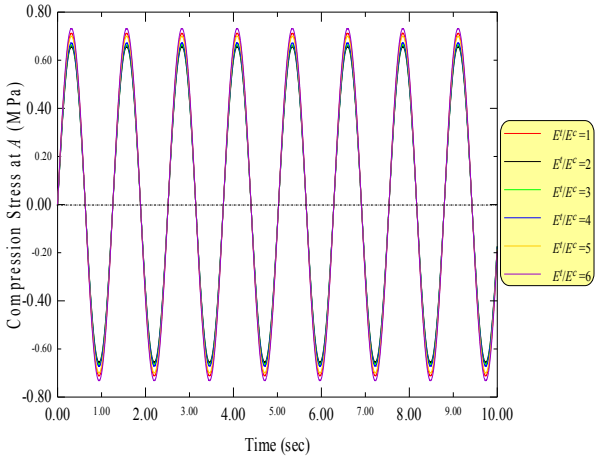

Figure (16): Time histories of the extreme-fibre compression stress for different E^t/E^c ratios.

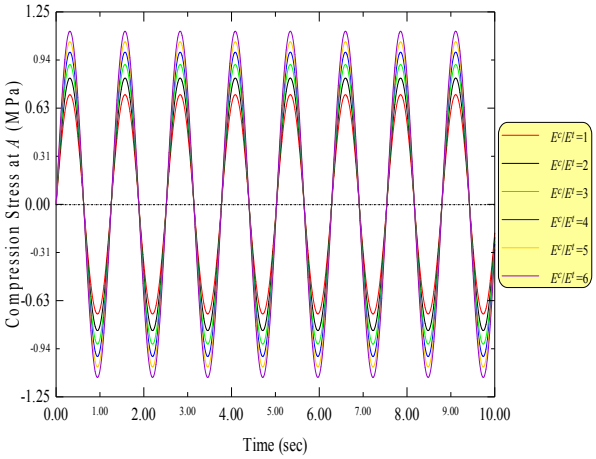

Figure (17): Time histories of the extreme-fibre compression stress for different E^c/E^t ratios.

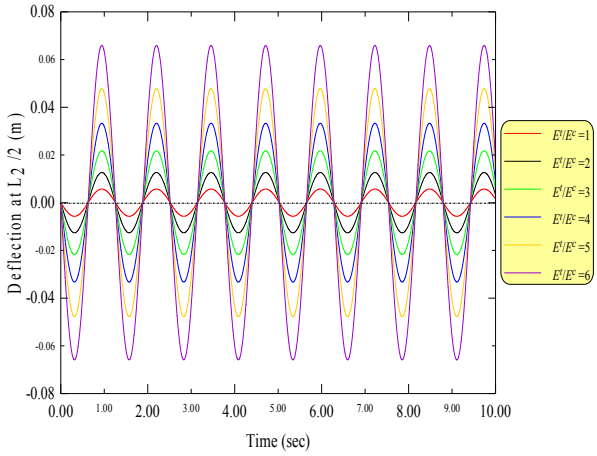

Figure (18): Time histories of the deflection at $L_2/2$ for different E^t/E^c ratios.

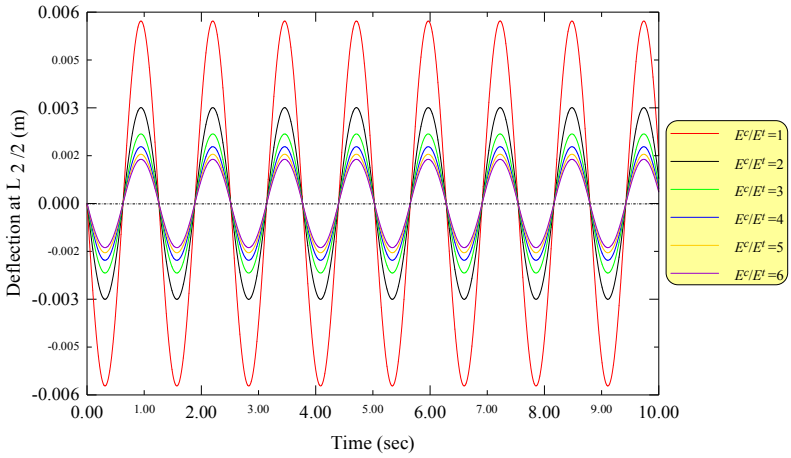

التحليل الحركي المعاد خطيا للعتبات ثنائية معامل المرونة

م.ناهض حماد كردي
قسم الهندسة المدنية
كلية الهندسة – جامعة الأنبار

عمر أحمد صالح
طالب ماجستير في قسم الهندسة المدنية
كلية الهندسة – جامعة الأنبار

الخلاصة.

نعرض في هذا البحث تحليلا حركيا حول خطيا للعتبات ثنائية معامل المرونة المعرضة للأحمال الجانبية. جُعِلَ موقع محور التعادل غير معتمد على أحداثيات المكان و الزمان بتبني فرض خاص حوّلَ المعادلة الحاكمة المشتبكة غير الخطية الى معادلة خطية غير مشتبكة. أصبح موقع محور التعادل بعدها دالة لهندسة المقطع و قيمتي معامل المرونة و استخرج بعدها بطريقة المقطع المكافئ. أشتقت مصفوفة الجسائة الحركية للعضو الواحد من دوال الشكل المضبوطة المحكومة بالمعادلة التفاضلية الجزئية الحاكمة و بنيت من هذه المصفوفة المصفوفة المناظرة للمنشأ بطريقة التجميع المعتادة في تحليل المنشئات. و حلت في هذا البحث أمثلة رمزية و عددية لتوضيح امكانية تطبيق الطريقة المقترحة و كفائتها.

الكلمات الرئيسية: التحليل الديناميكي،مادة ثنائية المعامل،طريقة المقطع المكافئ،مصفوفة القساوة الديناميكية،انفعال خطي،عتبة أويلر –برنولي.